Sensor for fisetin based on gold nanoparticles in ionic liquid and binuclear nickel complex immobilized in silica

Daniela Brondani,*[a] Iolanda Cruz Vieira,[a] Clovis Piovezan,[b] Jaqueline Maria Ramos da Silva,[b] Ademir Neves,[b] Jairton Dupont[c] and Carla Weber Scheeren[c]

Received 3rd December 2009, Accepted 19th February 2010
First published as an Advance Article on the web 1st March 2010
DOI: 10.1039/b925533h

Gold nanoparticles dispersed in an ionic liquid 1-butyl-3-methylimidazolium hexafluorophosphate (Au-BMI.PF_6) and a binuclear nickel(II) complex ([Ni_2(HBPPAMFF)μ-$(OAc)_2(H_2O)$]BPh_4) immobilized on functionalized silica were successfully applied in the construction of a novel sensor for the determination of fisetin by square-wave voltammetry. Under optimized conditions, the analytical curve showed two linear ranges for fisetin concentrations from 0.28 to 1.39 μM and 2.77 to 19.50 μM with a detection limit of 0.05 μM. This sensor demonstrated suitable stability (*ca.* 150 days; at least 500 determinations) and good repeatability and reproducibility, with relative standard deviations of 2.91 and 5.11%, respectively. The recovery study of fisetin in apple juice samples gave values from 96.4 to 106.4%. The efficient analytical performance of the proposed sensor can be attributed to the effective immobilization of the $Ni^{II}Ni^{II}$ complex on silica and the Au-BMI.PF_6 contribution to the electrode response.

Introduction

Flavonoids are a group of polyphenolic compounds found ubiquitously in plants, and they have broad pharmacological activity, alleged anti-ageing properties, and are subsequently used in a great variety of health products.[1,2] Fisetin (3,7,3′,4′-tetrahydroxyflavone), a naturally occurring flavonol, is a member of the flavonoids which has attracted attention because of its strong antioxidant properties and is suggested as a potentially useful therapeutic agent against various free radical-mediated diseases.[3–5] Fisetin is found in fruits and vegetables, such as strawberry, apple, grape, onion and cucumber. This polyhydroxyflavone is thought to be beneficial against various diseases including cancer, cardiovascular and neurodegenerative disorders (*e.g.* Alzheimer's disease).[6–8] Recently, Maher and co-authors[9] showed that fisetin enhances memory, and therefore it may be useful for treating patients with memory disorders.

Several analytical methods have recently been proposed for the determination of fisetin and other flavonoids, including high-performance liquid chromatography (HPLC),[10–13] capillary electrophoresis[10,11] and electrochemical methods.[14] Fang *et al.*[12] proposed a reversed-phase HPLC method for determination of flavonoids in red wine. The calibration curve for fisetin was linear over the range of 1.55–24.80 mg L^{-1} and the limit of detection was 14.6 μg L^{-1}. However, many of these conventional analytical methods are very expensive and require long execution times. The development of a sensor for voltammetric analysis is an attractive alternative for fisetin quantification because it offers important advantages including good sensitivity, fast response, no need for sample pretreatment, simplicity of construction and operation, cost-effectiveness and easy renovation of the surface.

Various sensors for the determination of phenolic compounds have been constructed employing electroactive mono- and polymetallic complexes.[15–18] The redox behavior of complexes which present catalytic activity toward important species is of great interest and has been attracting the attention of researchers for some time, due to the possibility of their application in sensor development. For example, de Oliveira *et al.*[17] presented a dinuclear iron complex, [$Fe^{III}Fe^{II}$(BPBPMP)$(OAc)_2$]ClO_4, containing the unsymmetrical ligand 2-bis[{(2-pyridylmethyl)-aminomethyl}-6-{(2-hydroxybenzyl)(2-pyridylmethyl)}-aminomethyl]-4-methylphenol (H_2BPBPMP), which has been described as being the first synthetic analogue for the redox properties of uteroferrin. This iron complex was employed in the construction of a new sensor for the determination of phenolic compounds by square-wave voltammetry. Recently, self-assembled monolayers of a nickel(II) complex and 3-mercaptopropionic acid on a gold electrode were obtained for determination of catechin in green tea, as described by Moccelini and co-workers.[18] This sensor exhibited a linear response for catechin concentrations from 3.31 to 25.30 μM and the detection limit was 0.826 μM.

Immobilization of transition-metal complexes by anchoring on solid supports has been the focus of a wide range of studies. These materials can be employed in areas such as catalysis and electroanalytical chemistry and, in particular, as electron-transfer mediators in molecular devices and multielectron transfer catalysis.[19,20] Among a series of important supports, silica is widely used as a supporting material because it presents advantageous properties such as high thermal, chemical and mechanical stability. In addition, the surface of silica can be chemically

[a]*Laboratory of Biosensors, Department of Chemistry, Universidade Federal de Santa Catarina, 88040-900 Florianópolis, SC, Brazil. E-mail: danielabrondani@hotmail.com*
[b]*Laboratory of Bioinorganic and Crystallography, Department of Chemistry, Universidade Federal de Santa Catarina, 88040-900 Florianópolis, SC, Brazil*
[c]*Laboratory of Molecular Catalysis, Institute of Chemistry, Universidade Federal do Rio Grande do Sul, 91501-970 Porto Alegre, RS, Brazil*

modified by attaching a great variety of pendant functional groups due to the presence of silanol groups.[19,21–23] These materials have been applied in the development of novel electrochemical sensors through the immobilization of electron mediator or electroactive species on the modified silica, incorporated especially in carbon-paste electrodes.[16,20,21]

In recent years, the study of nanoscale materials has been extensive, particularly with respect to metallic nanoparticles due to their unique chemical and physical characteristics compared with the bulk solids. Their catalytic activity, size controllability, high active surface area, chemical stability and attractive optical properties make them very useful in catalytic reactions and electroanalytical applications.[24–26] In particular, gold nanoparticles have been utilized progressively in the development of electrochemical sensors, increasing the sensitivity of the method to facilitate the electron transfer.[25,27–29] Franzoi and co-workers[29] developed novel biosensors based on silver or gold nanoparticles dispersed in ionic liquid (IL) and laccase immobilized in chitosan chemically crosslinked with cyanuric chloride. The proposed biosensors were employed in luteolin determination and the biosensor containing gold nanoparticles presented greater sensitivity.

In addition, ionic liquids (ILs) are gaining wide recognition as novel solvents in several areas of chemistry. The unusual properties of the ILs, such as high ionic conductivity, catalytic activity, negligible vapor pressure, and electrochemical and thermal stability[30,31] make them attractive materials for organic chemical reactions,[32] polymer synthesis and analytical applications.[33,34] In particular, they are widely used for the synthesis and stabilization of inorganic nanomaterials (*e.g.* metallic nanoparticles)[35,36] and the construction of modified electrodes.[37–39] In a study performed by Musameh and Wang,[37] ILs were used to prepare carbon paste electrodes with improved sensitivity, linearity, and stability.

In this study, gold nanoparticles dispersed in the ionic liquid 1-butyl-3-methylimidazolium hexafluorophosphate (Au-BMI.PF_6) and a binuclear nickel(II) complex ([Ni_2(HBPPAMFF)-μ-$(OAc)_2(H_2O)$]BPh_4) immobilized on 3-aminopropyl-functionalized silica were employed to develop a novel sensor for fisetin. The amount of nickel complex immobilized in the silica and Au nanoparticles in the IL (Au-BMI.PF_6) in the composition of the electrode, as well as the effect of the various operational parameters on the sensor response, were investigated in detail to obtain the best performance of the proposed sensor. The optimized sensor was then applied to fisetin determination in apple juice samples by square-wave voltammetry.

Experimental

Reagents and solutions

Fisetin was purchased from Aldrich and a standard solution (0.28 mM) was prepared daily in ethanol–water solution (40 : 60%, v/v). Rutin, caffeic acid, chlorogenic acid, catechin, quercetin, malic acid, fumaric acid, citric acid, oxalic acid, benzoic acid, ascorbic acid and 3-aminopropyl functionalized silica gel (particle size 40–63 μm and pore size 60 Å) were obtained from Sigma. All reagents were of analytical grade, used without further purification and all solutions were prepared with double-distilled water. Acetate buffer (0.1 M, pH 5.0) solution was used as the supporting electrolyte. The gold nanoparticles dispersed in the ionic liquid 1-butyl-3-methylimidazolium hexafluorophosphate (Au-BMI.PF_6) were synthesized as previously described in the literature.[40,41] Graphite powder (Acheson 38, Fisher Scientific) and Nujol (Aldrich) of high purity were used in the preparation of the carbon paste.

Synthesis and characterization of gold nanoparticles in ionic liquid BMI.PF_6

The Au-BMI.PF_6 was synthesized by placing $HAuCl_4 \cdot 3H_2O$ (10 mg; 25 mmol) dissolved in 0.5 mL of MeOH and dispersed in 0.5 mL of BMI.PF_6 ionic liquid in a Schlenk tube. The solution was stirred at room temperature for 15 min and 1-methylimidazole (5 μg; 0.06 mmol) was added. A solution containing $NaBH_4$ (9.25 mg; 250 mmol) was dissolved in 0.5 mL of MeOH, dispersed in 0.5 mL of BMI.PF_6 ionic liquid, 24 h before use. After stirring, the solution containing $NaBH_4$ in MeOH and BMI.PF_6 was added to the solution containing $HAuCl_4 \cdot 3H_2O$ in MeOH and BMI.PF_6, and a blue "solution" was obtained, and dried under reduced pressure.[41] The Au nanoparticles were isolated by centrifugation (3500 rpm) with the addition of 5.0 mL of acetone for 3 min and washed with acetone (3 × 15 mL) and dichloromethane (3 × 15 mL), dried under reduced pressure and isolated for the characterization of Au.BMIPF_6 by TEM analysis.

TEM analysis of the isolated Au-BMI.PF_6 nanoparticles was performed using a JEOL JEM1200EXII microscope operating at 120 kV. A 20 μm objective aperture and slightly under-focused ($4f \approx -300$ nm) objective lens were used to obtain the bright field TEM images. The histograms of the Au-BMI.PF_6 nanoparticle size distribution were obtained from measurements of around 300 diameters and were reproduced in different regions of the Cu grid.[42]

Synthesis and characterization of the ligand and $Ni^{II}Ni^{II}$ complex

The synthesis and characterization of the ligand and binuclear nickel(II) complex were thoroughly studied. The ligand 2-[(*N*-benzyl-*N*-2-pyridylmethylamine)]-4-methyl-6-[*N*-(2-pyridylmethyl)-aminomethyl]-4-methyl-6-formylphenol (H_2BPPAMFF) was characterized by ^{1}H NMR δ_H (400 MHz; $CDCl_3$): 10.2 [1H, aldehyde], 8.5 [2H, Py]; 7.6–6.8 [15H, Ar]; 3.8–3.6 [12H, CH_2], 2.2 [6H, CH_3] in ppm. CHN%($C_{37}H_{38}N_4O_3$) found (calc) C 75.2(75.7), H 6.1(6.5), N 9.5(9.2) melting point (57–62 °C). Yield: 70%. The complex [Ni_2(HBPPAMFF)μ-$(OAc)_2(H_2O)$]BPh_4 was synthesized in methanolic solution by mixing $Ni(ClO_4)_2 \cdot 6H_2O$ (0.73 g, 2 mmol, in 20 mL) and the H_2BPPAMFF ligand (0.58 g, 1 mmol, in 20 mL) with stirring and mild heating (60 °C). After 15 min, the $NaCH_3COO \cdot 3H_2O$ (0.16 g, 2 mmol) was added, and a green solution was obtained. $NaBPh_4$ (0.34 g, 1 mmol) was then added, and immediately a light green solid was formed, which was filtered off and dried under vacuum for 24 h. Yield: 58%. IR (KBr), in cm^{-1}: ν (C–H_{Ar} and C–H_{Aliph}) 3431 − 2922; ν (C=N and C=C) 1637–1427; ν_{ass} (OAc) 1552; ν_{sym} (OAc) 1479; ν(*H*–O_{phen}), 1375ν (C–O) 1263; δ (C–H_{Ar}) 734 and 705. CHN% Calc. for $Ni_2C_{65}H_{67}N_4O_8B$ (Found): C 67.2 (67.6); H 5.8 (5.7) N 4.8. Λ_M = 120 Ω^{-1} cm^2 mol^{-1} in CH_3CN electrolyte 1 : 1; Uv-vis

308 nm ($\varepsilon = 4300$ mol L^{-1} cm^{-1}), 390 nm ($\varepsilon = 4700$ mol L^{-1} cm^{-1}), 604 nm ($\varepsilon = 20$ mol L^{-1} cm^{-1}) in acetonitrile.

Immobilization of the $Ni^{II}Ni^{II}$ complex on functionalized silica

The 3-aminopropyl functionalized silica gel (extent of labeling ~1 mmol g^{-1} NH_2 loading, active group ~9% functionalized, matrix irregular silica particle platform, matrix active group NH_2 phase, particle size 40–63 μm, pore size 60 Å, surface area 550 m^2 g^{-1}) was used as the support for $Ni^{II}Ni^{II}$ complex immobilization. Briefly, a mass of 1.0 g of silica was suspended in 10 mL of acetonitrile under mild magnetic stirring, and 0.1 g (~86 μmol) of the complex $[Ni_2(HBPPAMFF)\mu\text{-}(OAc)_2(H_2O)]BPh_4$ diluted in a minimal amount of acetonitrile was added. After 24 h of reaction (at room temperature), the solid was filtered off and washed exhaustively with acetonitrile in a Soxhlet extractor for 12 h. The color of the silica became a strong light yellowish green, and the supernatant solution was stored quantitatively to determine the amount of $[Ni_2(HBPPAMFF)\mu\text{-}(OAc)_2(H_2O)]BPh_4$ immobilized on the support. The immobilized silica-complex product was finally dried at room temperature for 24 h, and characterized by IR, showing one weak band at 1630 cm^{-1} (νC=N) which indicated the formation of an imine bond. Other bands were revealed by the strong stretching vibrations of ν(Si–O) and solid-state UV-Vis (KBr pallets) at 442 nm, 478 nm and 640 nm.

Sensor construction

The sensor was constructed by mixing of the $Ni^{II}Ni^{II}$ complex immobilized on silica (7.5 mg; 5%, w/w) and graphite powder (75.0 mg; 60%, w/w) in a mortar for 20 min to ensure the uniform dispersion of the complex. Subsequently, Nujol (22.5 mg; 17.5%, w/w) and gold nanoparticles dispersed in $BMI.PF_6$ ionic liquid (22.5 mg; 17.5%, w/w) were added and mixed for at least 20 min to produce the final paste. The resulting modified carbon paste was packed into a plastic syringe (1.0 mm internal diameter) and a copper wire was inserted to obtain the external electric contact. The sensor without nanoparticles containing Nujol and mixtures of Nujol : $BMI.PF_6$ and the sensor of free nickel complex were prepared following the same steps. The bare carbon paste electrode (bare CPE) was prepared in a similar way by mixing graphite powder and Nujol in a mortar. The constructed electrodes were stored at room temperature in a dry place when not in use.

Instrumentation and electrochemical measurements

Square-wave voltammetry measurements using the sensor were performed on an Autolab PGSTAT12 potentiostat/galvanostat (Eco Chemie, Utrecht, The Netherlands) connected to data processing software (GPES, version 4.9.006, Eco Chemie). A conventional three-electrode system was used with a sensor based on gold nanoparticles dispersed in ionic liquid (Au-$BMI.PF_6$) and $Ni^{II}Ni^{II}$ complex immobilized on the support as the working electrode, a platinum wire as the counter electrode and an Ag/AgCl (3.0 M KCl) electrode as the reference electrode.

The general procedure used for electrochemical measurements was as follows: 10.0 mL aliquots of the acetate buffer solution (0.1 M; pH 5.0) at room temperature (25.0 ± 0.5 °C) were transferred to a clean dry cell and successive additions of fisetin or sample solutions were made using a micropipette. The square-wave voltammetry measurements were performed applying a sweep potential between +0.60 and −0.10 V, at frequency 10–100 Hz, pulse amplitude 10–100 mV and scan increment 1.0–12.0 mV, after successive additions of the analyte. All potentials were measured and reported *vs.* Ag/AgCl (3.0 M KCl), after a suitable initial stirring time of 60 s in order to homogenize the solution.

Preparation and analysis of apple juice samples

Four samples of apple juice were obtained from local supermarkets in Florianópolis (Santa Catarina, Brazil) and analyzed using the proposed sensor. The samples were prepared by dilution of apple juice in acetate buffer solution (0.1 M; pH 5.0) at room temperature (25.0 ± 0.5 °C), after which the solutions were filtered and homogenized for about 1 min, without the need for additional treatment of these samples. Aliquots of juice samples were transferred to an electrochemical cell and successive additions of fisetin standard solution were made using a micropipette. After each addition, square-wave voltammograms were recorded by scanning the potential from +0.60 to −0.10 V, at a frequency of 60 Hz, pulse amplitude of 100 mV and increment of 10.0 mV. All measurements were performed in triplicate.

Results and discussion

Characterization of Au nanoparticles in $BMI.PF_6$

The morphology and electron diffraction of the isolated Au-$BMI.PF_6$ nanoparticles were analyzed by TEM. The sample of Au-$BMI.PF_6$ was agitated ultrasonically and then deposited on holey carbon film supported by a copper grid. The grids were placed on filter paper to remove the excess material, allowed to dry out for 2 h under high vacuum and the samples examined. Bright field TEM observations were performed under slight under-focus conditions ($\Delta f \approx -300$ nm), and particle size distributions of the Au-$BMI.PF_6$ were determined once the original negative had been digitalized and expanded to 470 pixels cm^{-1} (Fig. 1-A). The particles display an irregular shape, but evaluation of their characteristic diameter results in a monomodal particle size distribution. A mean diameter of $d_m \approx 11 \pm 0.3$ nm of the Au-$BMI.PF_6$ nanoparticles was estimated from

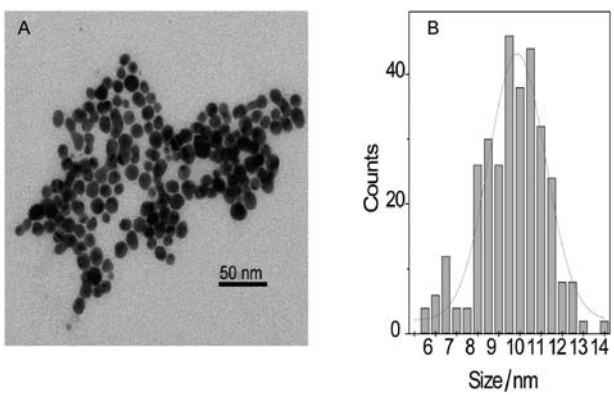

Fig. 1 TEM micrographs (A) and histograms (B) showing the particle size distribution of Au-$BMI.PF_6$.

ensembles of 300 particles, found in an arbitrarily chosen area of the enlarged micrographs. Fig. 1-B shows the particle size distributions obtained that can be reasonably well fitted by a Gaussian curve. The TEM analysis of the proposed sensor was carried out to verify the presence and dispersion of the Au-BMI.PF_6.

Cyclic voltammetry of the binuclear nickel complex

Complexes which are capable of mimicking the active site of different enzymes have been successfully used in the construction of novel sensors. In recent years, we have synthesized and characterized different structural and functional model complexes for the construction of sensors for the determination of phenolic compounds. These have shown high stability, performance and sensitivity.[17,18] In this paper, a novel binuclear nickel complex with high catalytic activity and affinity for diphenols was investigated.

This binuclear nickel complex was analyzed by cyclic voltammetry to investigate its electrochemical behavior. Fig. 2 shows the cyclic voltammogram for the nickel complex in acetonitrile and 0.1 mol L^{-1} tetrabutylammonium hexafluorphosphate performed by scanning the potential between −2.0 and −0.6 V *vs.* NHE at a scan rate of 100 mV s^{-1}. As can be seen, the complex shows two non-reversible cathodic waves at −1.27 and −1.64 V. These redox potentials can be attributed to the electron transfer processes $Ni^{II}Ni^{II} \rightarrow Ni^{II}Ni^{I}/Ni^{II}Ni^{I} \rightarrow Ni^{I}Ni^{I}$. The non-reversibility of these processes is indicative of the instability of the totally reduced form in solution.

$Ni^{II}Ni^{II}$ complex immobilized on silica and catalytic reaction

As in the case of several other research studies, silica materials were used as a supporting matrix because they present desirable properties such as mechanical and thermal resistance, which contribute to the efficiency of the immobilization. Also, the surface of silica can be functionalized with various organic moieties, by reaction of the silanol groups on the silica surface with chloro- and alkoxysilanes. Silica functionalized with 3-aminopropyl groups has diverse potential applications, such as in the development of adsorbents for heavy metals in wastewater treatment and supports for the immobilization of active transition metal ions or metallic complexes.[19–23,43] All of these characteristics indicate that this is a very suitable material for use as a support in the anchoring of the complex developed.

The immobilization of the $[Ni_2(HBPPAMFF)\mu\text{-}(OAc)_2\text{-}(H_2O)]BPh_4$ complex on 3-aminopropyl-functionalized silica was achieved through the reaction of aldehyde groups of the complex with amine groups of the functionalized silica, forming a covalent bond (Fig. 3). According to the characterization by IR, one weak band at 1630 cm^{-1} (νC=N) confirms the formation of an imine bond. The amount of $Ni^{II}Ni^{II}$ complex in the product obtained was approximately 37.2 μM of complex per g of silica.

Immobilization of metallic complexes by anchoring on the surface of solid supports (*e.g.* chemically-modified silica) is an area of great interest in current research on catalysts and electroanalytical chemistry.[19–21,23,43] These materials can be applied in several electrochemical reactions and have been successfully employed in the development of chemical sensors for phenolic compounds. Fig. 4-A shows the components used to fabricate the sensor, and the $Ni^{II}Ni^{II}$ complex catalyzes the oxidation of fisetin to its respective *o*-quinone and, subsequently, the quinone produced at the sensor surface is electrochemically reduced to fisetin at a potential of approximately +0.25 V *vs.* Ag/AgCl (as illustrated in Fig. 4-B).

The electrochemical behavior of fisetin using the bare CPE and the sensor based on the $Ni^{II}Ni^{II}$ complex was investigated by cyclic voltammetry. In this study, cyclic voltammetry measurements were obtained by sweeping the potential between +0.6 and 0.0 V *vs.* Ag/AgCl at a scan rate of 100 mV s^{-1}. Fig. 4-B shows the cyclic voltammograms obtained using the bare CPE (a and b) and Nujol : Au-BMI.PF_6-sensor (c and d) in 0.1 M acetate buffer solution (pH 5.0) and 0.5 mM standard solution fisetin, respectively. As can be observed, the response to the oxidation of fisetin to its corresponding *o*-quinone and the electrochemical reduction back to fisetin using the proposed sensor, due to the addition of the $Ni^{II}Ni^{II}$ complex, was much better than that of the bare CPE.

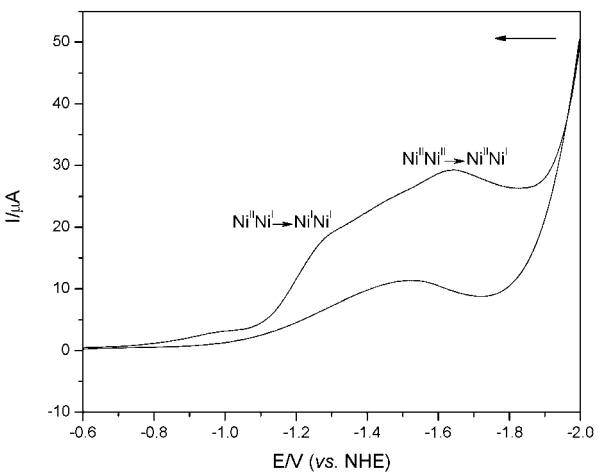

Fig. 2 Cyclic voltammogram of binuclear nickel complex in acetonitrile and 0.1 M tetrabutylammonium hexafluorophosphate performed by scanning the potential between −2.0 and −0.6 V *vs.* NHE, at a scan rate of 100 mV s^{-1}.

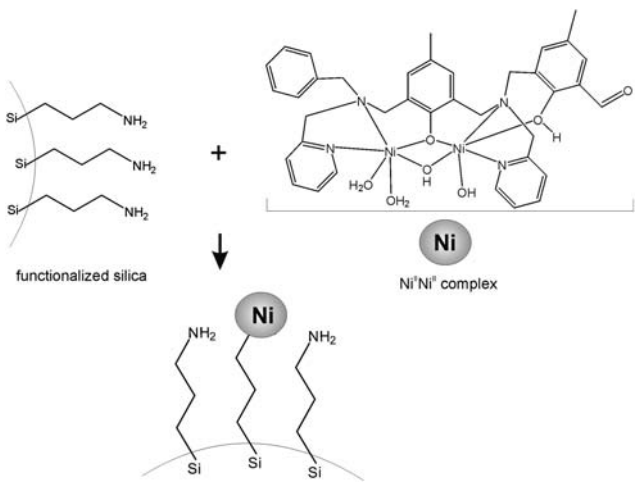

Fig. 3 Schematic representation of the immobilization of the $Ni^{II}Ni^{II}$ complex on the surface of 3-aminopropyl-functionalized silica.

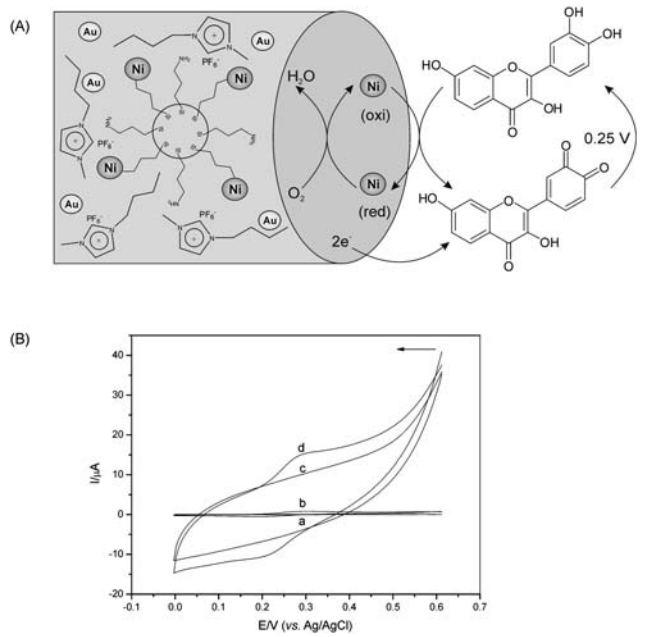

Fig. 4 (A) Schematic representation of the complex-catalyzed oxidation of fisetin with its subsequent electrochemical reduction on the sensor surface and components used for fabrication of the sensor. (B) Cyclic voltammograms obtained using the bare CPE (a and b) and Nujol : Au-BMI.PF_6-sensor (c and d) in 0.1 M acetate buffer solution (pH 5.0) and 0.5 mM standard solution of fisetin, respectively, at 100 mV s^{-1}.

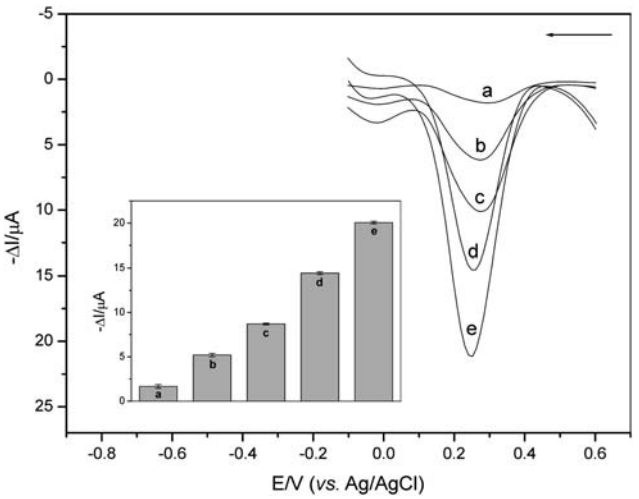

Fig. 5 Square-wave voltammograms obtained using the (a) bare CPE, (b) Nujol-sensor (free complex), (c) Nujol-sensor, (d) Nujol : BMI.PF_6-sensor, and (e) Nujol : Au-BMI.PF_6-sensor (c, d, and e – immobilized complex) in 10.8 μM fisetin in 0.1 M acetate buffer solution (pH 5.0); pulse amplitude 100 mV, frequency 60 Hz and scan increment 10.0 mV. Inset: cathodic peak current values for bare CPE and different sensors.

Application of $Ni^{II}Ni^{II}$ complex immobilized on silica and Au-BMI.PF_6 in sensor construction and voltammetric behavior

Different sensors were constructed using the $Ni^{II}Ni^{II}$ complex immobilized on silica and BMI.PF_6 ionic liquid containing gold nanoparticles in order to verify the contribution of these materials to the analytical response. The electrochemical behavior of fisetin using these sensors was investigated by square-wave voltammetry in the potential range of +0.60 to –0.10 V *vs.* Ag/AgCl. Fig. 5 shows the voltammograms obtained using the (a) bare CPE, (b) Nujol-sensor (free complex), (c) Nujol-sensor, (d) Nujol : BMI.PF_6-sensor, and (e) Nujol : Au-BMI.PF_6-sensor (c, d, and e – immobilized complex) in 10.8 μM fisetin in 0.1 M acetate buffer solution (pH 5.0); with pulse amplitude 100 mV, frequency 60 Hz and scan increment 10.0 mV. As can be observed, the Nujol-sensor (b) presented a response around three times larger than the bare CPE (a), due to the redox nature of the free $Ni^{II}Ni^{II}$ complex present in the electrode. However, the current for fisetin was approximately 40.2% higher in the presence of immobilized complex (c), showing that the efficient anchoring improved the analytical response. The cathodic peak current of the Nujol : BMI.PF_6-sensor (d) was increased in relation to the Nujol-sensor, due to the presence of the IL with a high ionic conductivity in the electrode. In addition, the differentiated viscosity of the employed ionic liquid contributes to the flow to the catalyst. This property (viscosity) is related to the conductivity, which is extremely important in electrochemical processes. The gold nanoparticles dispersed in ionic liquid (Au-BMI.PF_6) used in the sensor (e) contributed to significantly improving the current, corresponding to around 71.9% of the response of the sensor without nanoparticles (d). This was caused by the introduction of the metal nanoparticles,[29,44,45] which facilitate the electron transfer and have catalytic properties, improving the sensitivity of the selected sensor. Thus, the high catalytic activity of the gold nanoparticles contributed to enhancing the electrocatalytic activity of the nickel complex and amplified the analytical signal of the fisetin.

Optimization of the sensor construction and operational parameters

The effect of the Nujol : IL ratio (100 : 0; 75 : 25; 50 : 50; 25 : 75 and 0 : 100% (w/w)) was investigated and the sensor responses in the fisetin determination by square-wave voltammetry were compared (data not shown). As previously reported by our group,[29,38,39,45] the addition of ILs (of up to 50%) to a CPE modifies the microstructure of the paste, and the charge transfer resistance decreases and the charge transfer rate increases, due to high conductivity of the IL in comparison with other binders. Hence, the Nujol : BMI.PF_6 (or Nujol : Au- BMI.PF_6) ratio of 50 : 50% (w/w) was used for subsequent sensor construction and square-wave voltammetry analysis for the determination of fisetin.

In addition, the effect of the $Ni^{II}Ni^{II}$ complex, immobilized in silica in percentages of 1 to 20% (w/w), on the modified carbon paste electrode containing gold nanoparticles dispersed in IL (Au-BMI.PF_6) was also investigated. The cathodic peak current increased with increases in the complex composition up to 5.0% (w/w). Therefore, this complex concentration was selected for subsequent studies and a composition of 60 : 17.5 : 17.5 : 5% (w/w/w/w) graphite powder : Nujol : Au-BMI.PF_6 : $Ni^{II}Ni^{II}$ complex, respectively, was used in the construction of the proposed sensor.

After the optimization of the sensor construction, the operational parameters were evaluated, in triplicate, to obtain the best performance of this electrode. Initially, the effects of the different supporting electrolytes (and pH), including borate buffer

solution (pH 9.0–10.0), tris buffer solution (pH 7.0–9.0), phosphate buffer solution (pH 6.0–8.0) and acetate buffer solution (pH 4.0–5.5), in all of the solutions in a concentration of 0.1 M, were investigated by square-wave voltammetry. The best electroanalytical responses for fisetin were obtained in acetate buffer solution at pH 5.0.

Subsequently, the parameters of square-wave voltammetry were optimized for the best performance of the sensor under the same conditions cited above. Frequency (10–100 Hz), pulse amplitude (10–100 mV) and scan increment (1.0–12.0 mV) were investigated for determination of fisetin. Briefly, the optimized parameters can be summarized as follows: frequency 60 Hz; amplitude 100 mV and scan increment 10.0 mV. Table 1 summarizes the range over which each variable was investigated and the optimal value found. The best experimental conditions were selected for subsequent experiments.

Interference study

The presence of other electroactive compounds is expected to affect considerably the analytical signal. Therefore, several substances that may be present in apple juice were selected for this interference study: rutin, caffeic acid, chlorogenic acid, catechin, quercetin, malic acid, fumaric acid, citric acid, oxalic acid, benzoic acid and ascorbic acid. To evaluate the interference in the analytical response of the proposed sensor, the influence of these possible interferents in the determination of fisetin in apple juice was investigated in detail using solutions containing 10.0 μM of fisetin and adding various concentrations of an interfering substance. The ratios of the concentration of fisetin to that of each substance were fixed at 1 : 1, 1 : 5 and 1 : 10. The interference study was performed in triplicate, and the results obtained are listed in Table 2. The criterion for the tolerated concentration of each interfering substance was a relative change in the analytical signal corresponding only to the standard solution of fisetin and the signal of the fisetin solution comprising less than ± 5% of the coexisting interfering substances. None of the substances studied interfered significantly with the proposed sensor, that is, this electrode was able to determine the amount of fisetin in the presence of the potential interferents with good selectivity.

Repeatability, reproducibility and stability of the sensor

The repeatability of the reduction current (analytical response) obtained using the same sensor was examined in acetate buffer solution (0.1 M, pH 5.0) containing 10.8 μM fisetin. The relative standard deviation (R.S.D.) was 2.9% for ten successive measurements. The biosensor-to-biosensor reproducibility was also investigated considering five sensors prepared independently. A good reproducibility was obtained, with relative standard deviations of 5.1% for the proposed sensor.

The stability and lifetime of the sensor are important parameters in analytical determinations. Thus, these parameters were investigated for the proposed sensor stored at room temperature with measurements taken every 1–5 days, over a 150-day period (at least 500 determinations for each quantity of carbon paste used in the syringe). This electrode showed an excellent operational stability, obtaining a response of over 86% for 150 days, confirming the good stability of the $Ni^{II}Ni^{II}$ complex immobilized on functionalized silica.

Table 1 Optimization of the experimental parameters for the sensor

Parameter	Range studied	Optimal value
Nujol : Au-BMI.PF_6 (%, w/w)	100 : 0–0 : 100	50 : 50
$Ni^{II}Ni^{II}$ complex immobilized on silica (%, w/w)	1–20	5
Electrolyte support/pH	Borate buffer/9.0–10.0 Tris buffer/7.0–9.0 Phosphate buffer/6.0–8.0 Acetate buffer/4.0–5.5	Acetate buffer/5.0
Frequency/Hz	10–100	60
Pulse amplitude/mV	10–100	100
Scan increment/mV	1–12	10

Table 2 Possible interferences tested with proposed sensor

Interfering substance	Tolerated concentration/μM	Relative change on the analytical signal of fisetin[a] (%)
Rutin	100	2.29 ± 0.3
Caffeic acid	100	3.38 ± 0.1
Chlorogenic acid	100	2.80 ± 0.2
Catechin	50	4.05 ± 0.1
Quercetin	50	3.72 ± 0.2
Malic acid	100	NI[b]
Fumaric acid	100	NI[b]
Citric acid	100	0.45 ± 0.1
Oxalic acid	100	NI[b]
Benzoic acid	100	NI[b]
Ascorbic acid	100	1.27 ± 0.1

[a] n = 3. [b] NI = no interfering substance.

Analytical performance of biosensor

Fig. 6 shows the square wave voltammograms and the inset the analytical curve for fisetin obtained employing the proposed sensor under the optimized operational parameters. As can be seen, the cathodic peak current at approximately +0.25 V *vs.* Ag/AgCl increased with increasing fisetin concentration. The analytical curve showed two linear ranges and the corresponding regression equations are indicated:

(I) 0.28 to 1.39 μM ($-\Delta I = 0.36(\pm 0.11) + 6.42(\pm 0.12)$ [fisetin]; $R^2 = 0.9995$)

(II) 2.77 to 19.50 μM ($-\Delta I = 7.83(\pm 0.18) + 1.191(\pm 0.01)$ [fisetin]; $R^2 = 0.9997$)

where ΔI is the cathodic current peak (μA) and [fisetin] is the fisetin concentration (μM). The fact that the sensor presents two different linear ranges may be related to the saturation of the metallic center of the available complex on the surface of the electrode, with greater accessibility of the fisetin molecules to the catalyst at lower concentrations, while at higher concentrations there is a sensitivity decrease due to a probable impediment to the access of the larger number of molecules. This behavior was reproduced from sensor to sensor. Similar behavior has been described in the literature for other modified carbon paste electrodes (containing metallic catalysts or enzymes) for the determination phenolic compounds.[46,47] The detection limit (three times the signal blank/slope) of these data was 0.052 μM. The sensitivity of this sensor is greater than that of other sensors

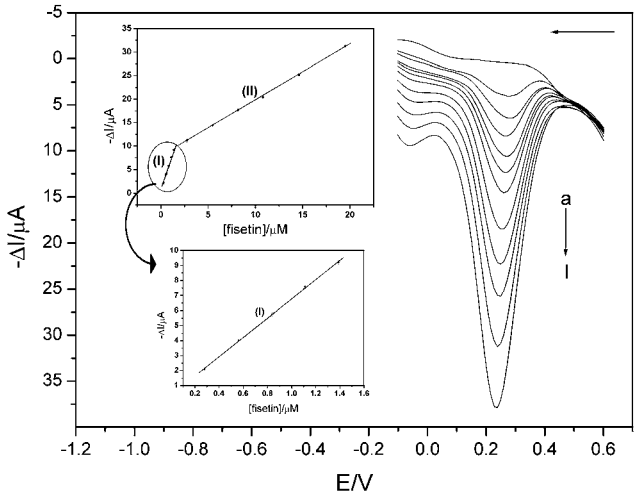

Fig. 6 Square wave voltammograms obtained using the proposed sensor for (a) blank in acetate buffer solution (0.1 M; pH 5.0) and fisetin solutions at the following concentrations: (b) 0.28; (c) 0.56; (d) 0.84; (e) 1.11; (f) 1.39; (g) 2.77; (h) 5.49; (i) 8.16; (j) 10.80; (k) 14.60 and (l) 19.50 μM at frequency 60 Hz, pulse amplitude 100 mV and scan increment 10.0 mV. Inset: analytical curve of fisetin.

constructed with nickel complexes, for the determination of phenolic compounds, described in the literature.[15,16,18] The satisfactory analytical performance of the proposed sensor can be attributed to the chemical stability and catalytic properties of the complex immobilized on silica, the high conductivity of the ionic liquid and the fact that the metal nanoparticles facilitate the electron transfer. This intrinsic catalytic contribution of each one of these materials contributes to significantly to improving the sensitivity.

Recovery study and analytical application

A recovery study and fisetin determination was performed by the standard addition method, in triplicate, using three commercial apple juice samples (A, B and C). Recovery measurements were obtained by adding different standard concentrations (8.0 to 32.0 μg 100 mL^{-1}) of fisetin to three juice samples. The percentage recovery values were calculated by comparing the concentrations detected in samples with and without the addition of known concentrations of the fisetin standard solution. The recoveries of 96.4 to 106.4% obtained for these samples demonstrate the satisfactory accuracy of the proposed sensor (Table 3). It can be clearly observed that the recovery results obtained indicate an absence of matrix effects in these determinations. In addition, to verify the efficiency of the developed sensor, these apple juice samples were used in the fisetin quantification. The fisetin contents determined in the samples A, B and C were 53.0, 151.0 and 41.0 μg 100 mL^{-1}, respectively (as shown in Table 3).

Conclusions

In this study, gold nanoparticles dispersed in an ionic liquid (Au-BMI.PF_6) and a binuclear nickel(II) complex immobilized on functionalized silica were successfully used in the construction of a novel sensor for the determination of fisetin in apple juice by square-wave voltammetry. This sensor exhibited high sensitivity, suitable selectivity, and good reproducibility and stability. The efficient analytical performance of the proposed sensor can be attributed to the effective immobilization of the $Ni^{II}Ni^{II}$ complex on silica and the high conductivity of the IL combined with the electron transfer facilitated by the metal nanoparticles. Additionally, the sensor was shown to be accurate, reliable, and quick to prepare through a low cost procedure, representing a satisfactory analytical method for the determination of fisetin in apple juice.

Table 3 Study of recovery and quantification of fisetin in apple juice using the proposed sensor

	Fisetin/μg 100 mL^{-1}		
Sample[a]	Added standard	Recovery[b]	Quantified[c]
A	8.0	99.3	53.0 ± 0.1
	16.0	104.8	
	24.0	103.5	
	32.0	96.4	
B	8.0	104.3	151.0 ± 0.5
	16.0	106.4	
	24.0	99.6	
	32.0	97.3	
C	8.0	97.9	41.0 ± 0.1
	16.0	99.5	
	24.0	100.5	

[a] A and B = commercial apple juice; C = fortified commercial apple juice. [b] Recovery = (found value mean/added value) x 100%. [c] Mean ± standard deviation; $n = 3$.

Acknowledgements

Financial support from CNPq (Processes 472169/2004-1 and 472541/2006-4), MCT/CNPq/PADCT, and also the scholarship granted by CAPES to DB are gratefully acknowledged.

References

1 N. C. Cook and S. Samman, *J. Nutr. Biochem.*, 1996, **7**, 66.
2 B. H. Havsteen, *Pharmacol. Ther.*, 2002, **96**, 67.
3 B. Sengupta, A. Banerjee and P. K. Sengupta, *FEBS Lett.*, 2004, **570**, 77.
4 B. Sengupta, A. Banerjee and P. K. Sengupta, *J. Photochem. Photobiol., B*, 2005, **80**, 79.
5 H.-H. Park, S. Lee, J.-M. Oh, M.-S. Lee, K.-H. Yoon, B. H. Park, J. W. Kim, H. Song and S.-H. Kim, *Pharmacol. Res.*, 2007, **55**, 31.
6 X. Lu, J. Jung, H. J. Cho, D. Y. Lim, H. S. Lee, H. S. Chun, D. Y. Kwon and J. H. Y. Park, *J. Nutr.*, 2005, **135**, 2884.
7 T.-W. Lian, L. Wang, Y.-H. Lo, I.-J. Huang and M.-J. Wu, *Biochim. Biophys. Acta: Mol. Cell Biol. Lipids*, 2008, **1781**, 601.
8 N. Khan, F. Afaq, D. N. Syed and H. Mukhtar, *Carcinogenesis*, 2008, **29**, 1049.
9 P. Maher, T. Akaishi and K. Abe, *Proc. Natl. Acad. Sci. U. S. A.*, 2006, **103**, 16568.
10 I. Molnár-Perl and Zs Füzfai, *J. Chromatogr., A*, 2005, **1073**, 201.
11 E. Rijke, P. Out, W. M. A. Niessen, F. Ariese, C. Gooijer and U. A. T. Brinkman, *J. Chromatogr., A*, 2006, **1112**, 31.
12 F. Fang, J.-M. Li, Q.-H. Pan and W.-D. Huang, *Food Chem.*, 2007, **101**, 428.
13 I. Novak, P. Janeiro, M. Seruga and A. M. Oliveira-Brett, *Anal. Chim. Acta*, 2008, **630**, 107.
14 G. J. Volikakis and C. E. Efstathiou, *Talanta*, 2000, **51**, 775.
15 J. Mohan, S. Joshi, R. Prakash and R. C. Srivastava, *Electroanalysis*, 2004, **16**, 572.

16 M. S. P. Francisco, W. S. Cardoso, L. T. Kubota and Y. Gushikem, *J. Electroanal. Chem.*, 2007, **602**, 29.
17 I. R. W. Z. de Oliveira, A. Neves and I. C. Vieira, *Sens. Actuators, B*, 2008, **129**, 424.
18 S. K. Moccelini, S. C. Fernandes, T. P. Camargo, A. Neves and I. C. Vieira, *Talanta*, 2009, **78**, 1063.
19 D. Brunel, N. Bellocq, P. Sutra, A. Cauvel, M. Laspéras, P. Moreau, F. D. Renzo, A. Galarneau and F. Fajula, *Coord. Chem. Rev.*, 1998, 1085.
20 L. Codognoto, P. G. Zanichelli and R. L. Sernaglia, *J. Braz. Chem. Soc.*, 2005, **16**, 620.
21 C. A. Borgo, R. T. Ferrari, L. M. S. Colpini, C. M. M. Costa, M. L. Baesso and A. C. Bento, *Anal. Chim. Acta*, 1999, **385**, 103.
22 M. Luechinger, R. Prins and G. D. Pirngruber, *Microporous Mesoporous Mater.*, 2005, **85**, 111.
23 F. G. Doro, U. P. Rodrigues-Filho and E. Tfouni, *J. Colloid Interface Sci.*, 2007, **307**, 405.
24 M. Pumera, S. Sánchez, I. Ichinose and J. Tang, *Sens. Actuators, B*, 2007, **123**, 1195.
25 X. Zhang, Q. Guo and D. Cui, *Sensors*, 2009, **9**, 1033.
26 F. W. Campbell and R. G. Compton, *Anal. Bioanal. Chem.*, 2010, **396**, 241.
27 S. Guo and E. Wang, *Anal. Chim. Acta*, 2007, **598**, 181.
28 F. Xiao, F. Zhao, J. Li, L. Liu and B. Zeng, *Electrochim. Acta*, 2008, **53**, 7781.
29 A. C. Franzoi, I. C. Vieira, J. Dupont, C. W. Scheeren and L. F. Oliveira, *Analyst*, 2009, **134**, 2320.
30 J. Dupont, *J. Braz. Chem. Soc.*, 2004, **15**, 341.
31 J. Dupont and P. A. Z. Suarez, *Phys. Chem. Chem. Phys.*, 2006, **8**, 2441.
32 T. Welton, *Coord. Chem. Rev.*, 2004, **248**, 2459.
33 J. Liu, J. A. Jönsson and G. Jiang, *Trends Anal. Chem.*, 2005, 24.
34 S. Pandey, *Anal. Chim. Acta*, 2006, **556**, 38.
35 Y. Zhou, *Curr. Nanosci.*, 2005, **1**, 35.
36 Z. Li, Z. Jia, Y. Luan and T. Mu, *Curr. Opin. Solid State Mater. Sci.*, 2008, **12**, 1.
37 M. Musameh and J. Wang, *Anal. Chim. Acta*, 2008, **606**, 45.
38 D. Brondani, J. Dupont, A. Spinelli and I. C. Vieira, *Sens. Actuators, B*, 2009, **138**, 236.
39 A. C. Franzoi, P. Migowski, J. Dupont and I. C. Vieira, *Anal. Chim. Acta*, 2009, **639**, 90.
40 C. C. Cassol, G. Ebeling, B. Ferrera and J. Dupont, *Adv. Synth. Catal.*, 2006, **348**, 243.
41 P. Dash and R. W. J Scott, *Chem. Commun.*, 2009, 812.
42 D. B. Williams and C. B. Carter, *Transmission Electron Microscopy, A Textbook for Materials Science*, Plenum, New York, 1996.
43 P. G. Zanichelli, R. L. Sernaglia and D. W. Franco, *Langmuir*, 2006, **22**, 203.
44 S. C. Fernandes, S. K. Moccelini, C. W. Scheeren, P. Migowski, J. Dupont, M. Heller, G. A. Micke and I. C. Vieira, *Talanta*, 2009, **79**, 222.
45 D. Brondani, C. W. Scheeren, J. Dupont and I. C. Vieira, *Sens. Actuators, B*, 2009, **140**, 252.
46 S. C. Fernandes, I. R. W. Z. de Oliveira, O. Fatibello-Filho, A. Spinelli and I. C. Vieira, *Sens. Actuators, B*, 2008, **133**, 202.
47 E. Shams, A. Babaei, A. R. Taheri and M. Kooshki, *Bioelectrochemistry*, 2009, **75**, 83.

